*Inorg. Chem.* **2003**, *42*, 6793–6800


# Speciation and Coordination Chemistry of Uranyl(VI)–Citrate Complexes in Aqueous Solution

**Sofie P. Pasilis and Jeanne E. Pemberton***

*University of Arizona, Department of Chemistry, Tucson, Arizona 85721*

Received February 17, 2003

The pH dependence of uranyl(VI) complexation by citric acid was investigated using Raman and attenuated total reflection FTIR spectroscopies and electrospray ionization mass spectrometry. pH-dependent changes in the $\nu_s(UO_2)$ envelope indicate that three major $UO_2^{2+}$–citrate complexes with progressively increasing U═O bond lengths are present over a range of pH from 2.0 to 9.5. The first species, which is the predominant form of uranyl(VI) from pH 3.0 to 5.0, contains two $UO_2^{2+}$ groups in spectroscopically equivalent coordination environments and corresponds to the $[(UO_2)_2Cit_2]^{2-}$ complex known to exist in this pH range. At pH values >6.5, $[(UO_2)_2Cit_2]^{2-}$ undergoes an interconversion to form $[(UO_2)_3Cit_3]^{3-}$ and $(UO_2)_3Cit_2$. ESI-MS studies on solutions of varying uranyl(VI)/citrate ratios, pH, and solution counteranion were successfully used to confirm complex stoichiometries. Uranyl and citrate concentrations investigated ranged from 0.50 to 50 mM.

## Introduction

Uranium contamination of soils at former Department of Energy nuclear fuel reprocessing facilities is a significant problem. Citric acid forms strong complexes with the uranyl(VI) ion and was used as a decontamination agent at these facilities. It is found as a component of mixed radioactive wastes[1] and occurs naturally in soils.[2] Due to its biodegradability and efficiency as a complexing agent, citric acid is currently being investigated for remediation of uranium-contaminated soils.[3−5] The presence of citric acid can influence both uranium speciation and extent of partitioning to mineral surfaces, affecting uranium mobility in the environment. Speciation and structural information on the $UO_2^{2+}$−citrate complexes is important to the development of mechanistic models describing adsorption phenomena affecting transport of uranium in soils and degradation pathways of these complexes. However, despite the investigation of $UO_2^{2+}$−citrate complexes over a 50-year period,[6−16] a complete understanding of speciation behavior is lacking, and little structural information is available.

The aqueous chemistry of the $UO_2^{2+}$−citrate system is complex, involving pH-dependent changes in stoichiometry and $UO_2^{2+}$ coordination environment. At low pH (pH 2−4), the existence of a 2:2 dimeric $UO_2^{2+}$−citrate species is well-established, and both the structure[12,13,15] (Figure 1a) and a formation constant[12,17] have been determined. A systematic study of the species formed at higher pH values has not previously been undertaken, and the studies that have been done have produced contradictory conclusions. Early potentiometric and spectrophotometric results suggested the pres-

* To whom correspondence should be addressed. E-mail: pembertn@email.arizona.edu. Phone: (520) 621-8245.

(1) Riley, R. G.; Zachara, J. M.; Wobbler, F. J. *Chemical contaminants on DOE lands and selection of contaminant mixtures for subsurface science research*; Technical Report, U.S. Department of Energy: Washington, DC, 1992.
(2) Huang, P. M.; Violante, A. In *Interactions of Soil Minerals with Natural Organics and Microbes*; Huang, P. M., Schnitzer, M., Eds.; Soil Science Society of America: Madison, WI, 1986; pp 159−221.
(3) Huang, J. W.; Blacklock, M. J.; Kapulnik, Y.; Ensley, B. D. *Environ. Sci. Technol.* **1998**, *32*, 2004−2008.
(4) Francis, A. J.; Dodge, C. J. *Environ. Sci. Technol.* **1998**, *32*, 3993−3998.
(5) Francis, C. W.; Thompson, M. E.; Wilson, J. H. *J. Hazard. Mater.* **1999**, *66*, 67−87.
(6) Feldman, I.; Neuman, W. F. *J. Am. Chem. Soc.* **1951**, *73*, 2312−2315.
(7) Neuman, W. F.; Havill, J. R.; Feldman, I. *J. Am. Chem. Soc.* **1951**, *73*, 3593−3595.
(8) Feldman, I.; Havill, J. R.; Neuman, W. F. *J. Am. Chem. Soc.* **1954**, *76*, 4726−4732.
(9) Heitner, C.; Bobtelsky, M. *Bull. Soc. Chim.* **1954**, *3*, 356−359.
(10) Gustafson, R. L.; Martell, A. E. *J. Am. Chem. Soc.* **1963**, *85*, 2571−2574.
(11) Feldman, I.; North, C. A.; Hunter, H. B. *J. Phys. Chem.* **1960**, *64*, 1224−1230.
(12) Rajan, K. S.; Martell, A. E. *Inorg. Chem.* **1965**, *4*, 462−469.
(13) Nunes, M. T.; Gil, V. M. S. *Inorg. Chim. Acta* **1987**, *129*, 283−287.
(14) Kakihana, M.; Nagumo, T.; Okamoto, M.; Kakihana, H. *J. Phys. Chem.* **1987**, *91*, 6128−6136.
(15) Allen, P. G.; Shuh, D. K.; Bucher, J. J.; Edelstein, N. M.; Reich, T.; Denecke, M. A.; Nitsche, H. *Inorg. Chem.* **1996**, *35*, 784−787.
(16) Lenhart, J. J.; Cabaniss, S. E.; MacCarthy, P.; Honeyman, B. D. *Radiochim. Acta* **2000**, *88*, 345−353.
(17) Martell, A. E.; Smith, R. M. *Critical Stability Constants. Vol 3. Other Organic Ligands*; Plenum Press: New York, 1982.

10.1021/ic0341800 CCC: $25.00 
Published on Web 09/18/2003

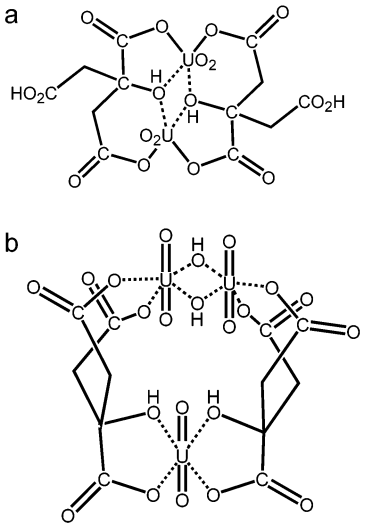


**Figure 1.** (a) Structure proposed for the 2:2 uranyl/citrate species (shown here in its completely protonated form).[12,13,15] (b) Structure proposed for the 3:2 uranyl/citrate species in ref 13.

ence of two trinuclear complexes with stoichiometries of 3:2 and 3:3 (ratios given throughout as uranyl/citrate) above a pH of ~7,[8] although a hexameric $UO_2^{2+}$−citrate complex was also proposed.[12] A later study using $^1H$ and $^{13}C$ NMR indicated the existence of only a 3:2 uranyl/citrate complex with a cyclic structure involving two hydroxo bridges at pH 8 (Figure 1b).[13] A straight-chain structure for a 3:2 complex at an unspecified pH was also suggested from $^{13}C$ NMR.[14] Knowledge of the $UO_2^{2+}$−citrate system at environmentally relevant pH values is important both for soil remediation and for understanding the effect of citrate on the mobility of uranyl in the environment.

The purpose of this study is to characterize the $UO_2^{2+}$−citrate complexes formed in aqueous solution and to gain an understanding of their speciation behavior. Here we present a systematic investigation of the $UO_2^{2+}$−citrate complexes using Raman and attenuated total reflectance FTIR (ATR-FTIR) spectroscopies and electrospray ionization mass spectrometry (ESI-MS). These tools provide complementary information and together offer a powerful approach for characterization of the solution behavior of inorganic complexes. The Raman-active $\nu_s(UO_2)$ mode and the IR-active $\nu_{as}(UO_2)$ mode are sensitive to changes in $UO_2^{2+}$ coordination environment and have been used to study uranyl complexation with various inorganic and organic ligands in aqueous solution.[18−24] Complexation of the uranyl(VI) ion weakens the O═U═O bonds, increasing bond lengths and causing shifts to lower frequency of the Raman-active $\nu_s(UO_2)$ and the IR-active $\nu_{as}(UO_2)$ modes. The extent of the shift is related to the stability of the complexing ligand. The strength of the $\nu_s(UO_2)$ mode and its sensitivity to changes in $UO_2^{2+}$ coordination environment make it particularly valuable for following the speciation of the $UO_2^{2+}$−citrate complexes. IR spectroscopy provides information on the conformation of the coordinating citrate ligand, while ESI-MS can be used to characterize the stoichiometries of the $UO_2^{2+}$−citrate complexes, as well as to corroborate speciation information obtained from Raman spectroscopy.

## Experimental Section

**Materials.** Citric acid (Aldrich, 99.5%), uranyl nitrate (Fluka, 98−102%), and uranyl chloride (All-Chemie LTD) were used as received. Water was purified with a Milli-Q UV system (Millipore Corp.). Ammonium hydroxide (Fluka, >99%) was used for pH adjustment of samples for Raman and ESI-MS measurements, while potassium hydroxide (Aldrich, 99.99%) was used for pH adjustment of samples prepared for ATR-FTIR measurements. Acetonitrile (EM Science, 99.8 or 99.99%) was used to prepare samples for ESI-MS measurements.

**Sample Preparation.** Solutions of 100 mM citric acid and 100 mM uranyl nitrate were prepared in 18 MΩ Milli-Q water. For Raman spectrochemical titrations, 30 mL each of the citric acid and uranyl nitrate solutions were added to a beaker. pH was adjusted upward using $NH_4OH$, and spectra were acquired after each addition of base. Samples were kept in the dark and under $N_2$ during analysis. For other Raman and for ATR-FTIR analyses, solutions of 100 mM citric acid and 100 mM uranyl nitrate were combined in the appropriate ratio, and pH was adjusted with $NH_4OH$ or KOH. Samples were kept in the dark during sample preparation and analysis. Samples for ESI-MS were prepared as above, brought to the appropriate pH with $NH_4OH$, and diluted to a concentration of 0.5 mM with a 20% (v/v) solution of acetonitrile−water. Uranyl chloride was sometimes used in place of uranyl nitrate in order to examine the effect of counteranion on adduct formation. pH was readjusted with $NH_4OH$ where necessary. pH measurements of the 20% (v/v) acetonitrile−water solutions were made using an electrode calibrated with aqueous buffers and are reported as ${}^{s}_{w}pH$. The ${}^{s}_{w}pH$ and the ${}^{s}_{s}pH$ scales are related through the relationship ${}^{s}_{s}pH = {}^{s}_{w}pH - \delta$, where $\delta = -0.02$ for a 20% (v/v) solution of acetonitrile/$H_2O$.[25] All pH measurements in this study were made using a Ross combination glass/reference electrode (Orion 8102) standardized against pH 1.68, 4, 7, and 10 buffers traceable to the NIST pH activity scale.

**Instrumentation.** Raman spectra were acquired using 75 mW of 532.06 nm radiation from a Coherent Verdi Nd:$YVO_4$ laser on a Spex 1877 Triplemate Spectrograph equipped with 600 gr/mm gratings in the filter stage and a 1200 gr/mm grating in the spectrograph stage. The entrance slit of the spectrometer was set at 0.5 mm, the slit at the filter stage was 7.0 mm, and the slit to the spectrograph stage was 50 $\mu$m for a spectral band-pass of 2.5 $cm^{-1}$. Scattered radiation was collected at 90° with respect to the exciting laser beam. The detector in these experiments was a Princeton Instruments charge-coupled device (CCD) system based on a RTE−1100-PB CCD of pixel format 1100 × 330, cooled by liquid $N_2$ to −90 ° C. Raman spectra were generally acquired on samples contained in sealed NMR tubes. Raman spectrochemical titration data were acquired in a continuous flow mode on samples pumped through an NMR tube. Raman spectra have a precision of ±2 $cm^{-1}$ or better and were calibrated using neon emission lines.

(18) Brooker, M. H.; Huang, C.-H.; Sylwestrowicz, J. *J. Inorg. Nucl. Chem.* **1980**, *42*, 1431−1440.
(19) Toth, L. M.; Begun, G. M. *J. Phys. Chem.* **1981**, *85*, 547−549.
(20) Gal, M.; Goggin, P. L.; Mink, J. *Spectrochim. Acta* **1992**, *48A*, 121−132.
(21) Nguyen-Trung, C.; Begun, G. M.; Palmer, D. A. *Inorg. Chem.* **1992**, *31*, 5280−5287.
(22) Quiles, F.; Burneau, A. *Vib. Spectrosc.* **1998**, *18*, 61−75.
(23) Quiles, F.; Burneau, A. *Vib. Spectrosc.* **2000**, *23*, 231−241.
(24) Nguyen-Trung, C.; Palmer, D. A.; Begun, G. M.; Peiffert, C.; Mesmer, R. E. *J. Solution Chem.* **2000**, *29*, 101−129.
(25) Espinosa, S.; Bosch, E.; Roses, M. *Anal. Chem.* **2000**, *72*, 5193−5200.

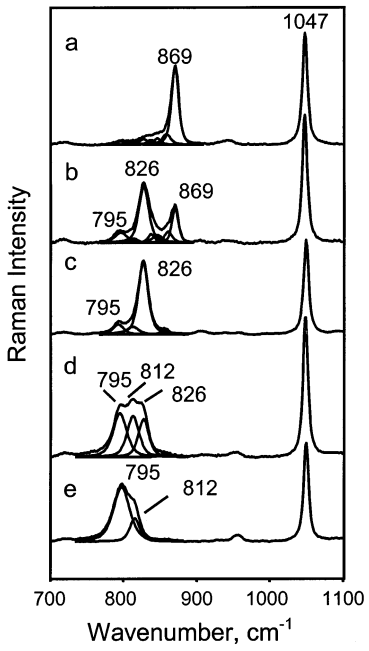


**Figure 2.** Raman spectra showing the pH dependence of $\nu_s(UO_2)$ at a uranyl/citrate ratio of 1:1 at (a) pH 1.6, (b) pH 2.1, (c) pH 3.4, (d) pH 5.4, (e) pH 8.5. All spectra acquired with 20 min integrations.

ESI-MS measurements were made using a Finnigan LCQ HPLC/MS instrument (Finnigan Co., San Jose, CA) using the sample solvent as a carrier. Samples were introduced using direct infusion with a flow rate of 13 $\mu$L/min. All experiments were performed in positive ion mode at the following electrospray ionization conditions: spray voltage, 4.57 kV; capillary voltage 40 V; capillary temperature, 200 °C; sheath gas, $N_2$; flow rate, 60 (arbitrary units).

ATR-FTIR spectra were acquired on a Nicolet Magna 550 series II spectrometer equipped with a liquid-$N_2$ cooled MCT detector. ATR-FTIR measurements were performed using a Twin Parallel Mirror Reflectance Attachment (TMPA) (Harrick Scientific Corporation) set at 45°. A Teflon internal reflection liquid cell (Harrick Scientific Corporation) was used for all ATR measurements. A 50 × 10 mm 45° ZnSe parallelogram ATR optical crystal was used as the reflectance medium. ATR-FTIR spectra were acquired using 1000 coadded scans of both sample and reference at 2 $cm^{-1}$ resolution with Happ-Genzel apodization.

**Peak Fitting.** GRAMS/32 was used for decomposition of Raman spectra. The peak fitting application in GRAMS/32 is based on the Levenberg−Marquardt method of nonlinear least-squares fitting for decomposition of overlapping peaks. The solution is considered to have converged when the reduced $\chi^2$ was minimized and the calculated peak envelope closely matched the experimental peak envelope. A 50:50 mixture of Gaussian and Lorentzian line shapes was used for peak fitting, as this appeared to fit the data more closely than either pure Gaussian or pure Lorentzian models.

## Results and Discussion

**Speciation.** Spectrochemical titrations were performed to determine the pH dependence of $UO_2^{2+}$−citrate complex formation. Figure 2a−e shows Raman spectra of a 1:1 solution of uranyl and citrate (50 mM in each) acquired as a function of pH. The vibrational band at 1047 $cm^{-1}$ is due to the $\nu_1(NO_3)$ mode, and since solutions were prepared using uranyl nitrate, is a constant feature in the spectra. Four major Raman bands appear successively with increasing pH in the region of the $\nu_s(UO_2)$ between 750 and 870 $cm^{-1}$. At pH 1.6 (Figure 2a), an intense band due to the solvated cation $UO_2(OH_2)_5^{2+}$, appears at 869 $cm^{-1}$. A series of small overlapping bands can be resolved by peak fitting at 858, 845, 836, 826, 812, and 795 $cm^{-1}$. The band at 858 $cm^{-1}$ may contain contributions from the hydrolyzed uranyl species $(UO_2)_2(OH)^{3+}$ and $(UO_2)_2(OH)_2^{2+}$, while the band at 836 $cm^{-1}$ is assigned to $(UO_2)_3(OH)_5^{+}$.[24] The band at 845 $cm^{-1}$ is assigned to another hydrolyzed uranyl species, $UO_2OH^+$, predicted to occur at 848 $cm^{-1}$,[24] although $\gamma_s$(COO) of citric acid also appears in this region. The bands at 826, 812, and 795 $cm^{-1}$ are assigned to three distinct $UO_2^{2+}$−citrate complexes, as discussed in following paragraphs.

At pH 2.1 (Figure 2b), the intensity of the $\nu_s(UO_2)$ band at 869 $cm^{-1}$ associated with the $UO_2(OH_2)_5^{2+}$ species decreases dramatically with a concomitant increase in the intensity of the Raman band at 826 $cm^{-1}$. This band is assigned to the 2:2 complex, $[(UO_2)_2Cit_2]^{2-}$ (Figure 1), initially inferred from potentiometric titration data[12] and confirmed by NMR[13] and EXAFS.[15] (For ease of discussion, "Cit" is used here to refer to the citrate trianion, $C_6H_5O_7^{3-}$.) The uranyl moieties in this complex are in equivalent coordination environments and give rise to a single $\nu_s(UO_2)$ band. There is no strong Raman evidence for either the 2:1 $UO_2^{2+}$−citrate complex or the mononuclear $UO_2^{2+}$−citrate complex variously proposed to coexist with the 2:2 complex.[12,13] However, it is possible that these species exist at concentrations below the limit of detection of Raman spectroscopy. Raman bands associated with hydrolyzed $UO_2^{2+}$ complexes increase slightly in intensity at pH 2.1, but citrate, as the stronger ligand, effectively competes with $OH^-$ for the uranyl ion, preventing the formation of insoluble mineral phases. Bands at 795 and 812 $cm^{-1}$ increase slightly in intensity at this pH and indicate that more highly oligomerized $UO_2^{2+}$−citrate complexes form as pH increases.

At pH 3.4, the bands for $UO_2(OH_2)_5^{2+}$, $(UO_2)_2(OH)^{3+}$, and $(UO_2)_2(OH)_2^{2+}$ disappear completely, and $[(UO_2)_2Cit_2]^{2-}$ becomes the predominant species in solution (Figure 2c). Upon further increase in pH, the 812 and 795 $cm^{-1}$ bands increase dramatically in intensity, while the band for $[(UO_2)_2Cit_2]^{2-}$ begins to systematically decrease before disappearing completely at pH > 8.5. The absence of Raman bands at 835 and 822 $cm^{-1}$ indicates that citrate complexes uranyl more strongly than $OH^-$ even at relatively high pH, effectively preventing the formation of significant concentrations of $(UO_2)_3(OH)_5^{+}$ and $(UO_2)_3(OH)_7^{-}$, species that would be expected at pH > 5.[24,26]

Feldman et al. concluded on the basis of potentiometric and spectrophotometric studies that $[(UO_2)_2Cit_2]^{2-}$ undergoes a reaction at higher pH to form complexes containing uranyl and citrate groups with stoichiometries of 3:3 ($[(UO_2)_3Cit_3]^{3-}$), and 3:2 ($(UO_2)_3Cit_2$), respectively.[8] In order to determine whether the two Raman bands at 812 and 795 $cm^{-1}$ are indeed related to the 3:3 and 3:2 $UO_2^{2+}$−citrate species, we repeated part of the original study of these researchers by

(26) Palmer, D. A.; Nguyen-Trung, C. *J. Solution Chem.* **1995**, *24*, 1281−1291.

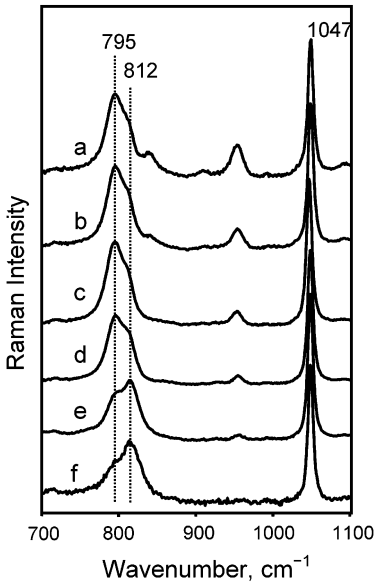


**Figure 3.** Method of continuous variations showing dependence of $\nu_s(UO_2)$ intensity on mole ratio of uranyl/citrate, pH 7.5: (a) 0.25, (b) 0.43, (c) 0.67, (d) 1.0, (e) 1.5, (f) 2.3.

using the method of continuous variation with Raman spectroscopy to reaffirm complex stoichiometries and to distinguish the Raman bands associated with each complex. Figure 3a−f shows the effect of varying uranyl/citrate ratios in solution at a constant pH of 7.6. It is clear that the species associated with the $\nu_s(UO_2)$ at 795 cm$^{-1}$ predominates at uranyl/citrate ratios of 1.0 and lower, while the species associated with the $\nu_s(UO_2)$ at 812 cm$^{-1}$ predominates at uranyl/citrate ratios of 1.5 and higher. The Raman band at 812 cm$^{-1}$ is therefore tentatively assigned to a species containing a 3:2 stoichiometry (uranyl/citrate), $(UO_2)_3Cit_2$; however, the Raman band at 795 cm$^{-1}$ cannot be definitely assigned to $[(UO_2)_3Cit_3]^{3-}$ from these data, although on the basis of the lower frequency of this mode relative to that for the $(UO_2)_3Cit_2$ species, it can be ascertained that this species is more highly oligomerized than either $[(UO_2)_2Cit_2]^{2-}$ or $(UO_2)_3Cit_2$. At a uranyl/citrate ratio of 2.3 and higher, a yellow material with a broad $\nu_{as}(UO_2)$ band centered at ~870 cm$^{-1}$ and with $\nu_s(UO_2)$ at ~ 820 cm$^{-1}$ forms in solution. This material is most likely a mixture of the α-, *β*-, and *γ*-$[UO_2(OH)_2]$ phases.[27]

In Figure 4, Raman spectrochemical titration data are presented to allow examination of the distribution of $UO_2^{2+}$−citrate species as a function of pH for a solution 50 mM each in uranyl and citrate. Band area (*A*) was determined through decomposition of the $\nu_s(UO_2)$ envelope and normalized to the $\nu_1(NO_3)$ band area ($A[\nu_{s(UO_2)}]/A[\nu_{1(NO_3)}]$) to compensate for changes in uranyl concentration and collection efficiency during the titration. The intense $\nu_1(NO_3)$ band is an ideal internal standard because $UO_2(OH_2)_5^{2+}$ and $NO_3^-$ form only a very weak ion pair, and because $NO_3^-$ is not perturbed by $UO_2^{2+}$−citrate complex formation. The titration was repeated 3 times, and 2−3 normalized band areas were averaged per data point; error bars represent the range of

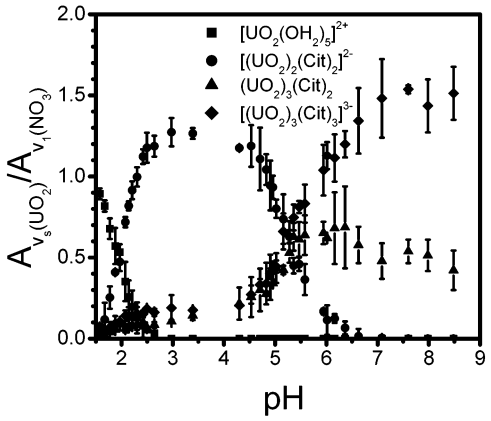


**Figure 4.** Raman spectrochemical titration showing $UO_2^{2+}$−citrate speciation as a function of pH.

normalized area values determined (pH scale error bars are smaller than the symbols). For clarity of presentation, hydrolyzed $UO_2^{2+}$ species present in low concentrations are omitted from the plot in Figure 4. The overall increase in normalized band area with pH is due to an increase in the Raman scattering cross-section of the uranyl moiety with extent of complexation. This phenomenon has previously been noted for $UO_2^{2+}$−sulfate and $UO_2^{2+}$−acetate complexes[22,28] and may be related to an increase in the polarizability of the O═U═O bond upon complexation.

Figure 4 cannot be strictly viewed as a speciation diagram, because the difficulties inherent in determining Raman scattering cross-sections for each species make it impossible to directly correlate peak areas with concentration. Given the known decrease in $\nu_s(UO_2)$ frequency with increase in O═U═O bond length, and increase in uranyl polarizability with increasing extent of complexation, Raman scattering cross-section should increase in the order $UO_2(OH_2)_5^{2+}$ < $[(UO_2)_2Cit_2]^{2-}$ < $(UO_2)_3Cit_2$ < $[(UO_2)_3Cit_3]^{3-}$. A dramatic increase in the area of the $[(UO_2)_2Cit_2]^{2-}$ band at 826 cm$^{-1}$ relative to that of the $UO_2(OH_2)_5^{2+}$ band at 869 cm$^{-1}$ between pH values of 1.5 and 2.5 lends support to this argument. In a similar fashion, the Raman scattering cross-section of $[(UO_2)_3Cit_3]^{3-}$ is predicted to be greater than that of $(UO_2)_3Cit_2$. Despite these changes in Raman scattering cross-section, this diagram does provide insight into the relative importance of each species in solution and is still useful as a qualitative guide to the pH-dependent behavior of the $UO_2^{2+}$−citrate complexes for the 1:1 uranyl/citrate system.

The dimeric $[(UO_2)_2Cit_2]^{2-}$ complex (Figure 1) is clearly the most stable of the three $UO_2^{2+}$−citrate species in the low pH region of the titration (pH < 4). Its formation begins at pH < 2, and it exists in equilibrium with small amounts of $(UO_2)_3Cit_2$ and $[(UO_2)_3Cit_3]^{3-}$. The $[(UO_2)_2Cit_2]^{2-}$ complex contains two ionizable COOH groups (Figure 1), which may explain its ability to further complex uranyl and interconvert to the $(UO_2)_3Cit_2$ and $[(UO_2)_3Cit_3]^{3-}$ species at pH > 4.5. Within the constraints of peak fitting, these latter two species exist at approximately equivalent concentrations at pH < 5. Between pH 5 and 6, $[(UO_2)_3Cit_3]^{3-}$ becomes

(27) Hoekstra, H. R.; Siegal, S. *J. Inorg. Nucl. Chem.* **1973**, *35*, 761−779.

(28) Burneau, A.; Tazi, M.; Bouzat, G. *Talanta* **1992**, *39*, 743−748.

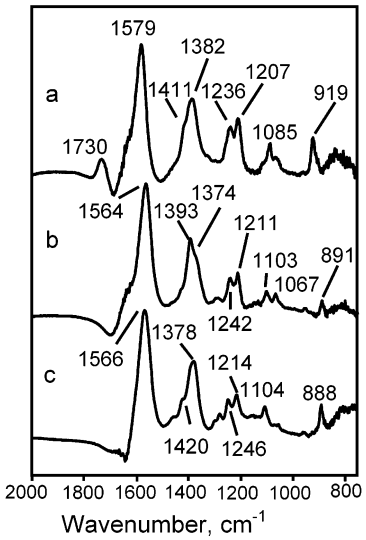


**Figure 5.** ATR-FTIR spectra showing spectral changes in citrate modes and $\nu_{as}(UO_2)$ as a function of pH and uranyl/citrate ratio: (a) pH 4.1, 1:1 uranyl/citrate, (b) pH 7.8, 1:1 uranyl/citrate, (c) pH 7.6, 3:2 uranyl/citrate.

increasingly dominant compared to $(UO_2)_3Cit_2$. Above pH 6, the concentration of $(UO_2)_3Cit_2$ decreases slightly relative to $[(UO_2)_3Cit_3]^{3-}$.

In contrast to the behavior observed in a solution containing equimolar amounts of uranyl and citrate, in a solution containing a 3:2 mole ratio of uranyl/citrate, the relative proportions of $(UO_2)_3Cit_2$ and $[(UO_2)_3Cit_3]^{3-}$ at pH > 6.5 are reversed from those already described (see for example Figure 3e,f). Nonetheless, the general trend in solution behavior is the same, with $(UO_2)_3Cit_2$ reacting to form $[(UO_2)_3Cit_3]^{3-}$ as pH is increased. Interestingly, no precipitate is observed under these solution conditions, even at pH 10, indicating that uranyl remains in solution as a citrate complex. On the basis of these results, the relevant solution equilibria with increasing pH can be represented schematically by

$$6UO_2^{2+}(aq) + 6[Cit]^{3-} \rightleftharpoons 3[(UO_2)_2Cit_2]^{2-} \rightleftharpoons 2(UO_2)_3Cit_2 + 2[Cit]^{3-} \rightleftharpoons 2[(UO_2)_3Cit_3]^{3-}$$

**ATR-FTIR Spectroscopy.** Figure 5 shows ATR-FTIR spectra of solutions containing 50 mM each of uranyl and citrate at pH 4.1 and 7.8 and of a solution 60 mM in uranyl and 40 mM in citrate at pH 7.6. At each of these pH values and uranyl/citrate ratios, one of the three major species in solution is expected to predominate.

In order to provide a basis for comparison of the vibrational behavior of uncomplexed and complexed citrate, ATR spectra of 100 mM solutions of citric acid and its mono-, di-, and trianions are shown in Figure 6a−d. Peak assignments are given in Table 1. The spectrum of fully protonated citric acid at pH 2.1 is characterized by two strong absorbance bands, the carbonyl symmetric stretching, $\nu_s$(C═O) at 1724 cm$^{-1}$, and a band at 1223 cm$^{-1}$ due to a combination of $\nu$(OC−OH) and $\delta$(C−O−H) modes of the carboxylic acid group. With the deprotonation of one COOH group at pH 4.0, both modes decrease in intensity and shift

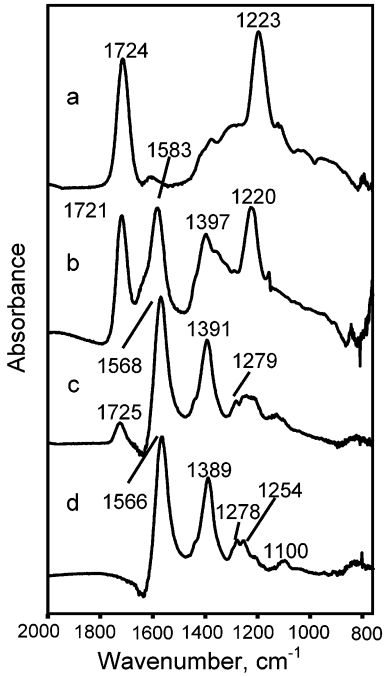


**Figure 6.** ATR-FTIR spectra of a 100 mM solution of citric acid showing spectral changes as a function of pH: (a) pH 2.1, (b) pH 4.0, (c) pH 5.5, (d) pH 7.8.

slightly to lower frequency, while two new modes appear at 1583 and 1397 cm$^{-1}$ that are assigned to the $\nu_{as}(COO^-)$ and $\nu_s(COO^-)$ modes, respectively. The spectra of the citrate dianion at pH 5.5 and the trianion at pH 7.8 are very similar in appearance, with the $\nu_{as}(COO^-)$ mode more intense than that of the monoanion and shifted to lower frequency by ∼20 cm$^{-1}$ relative to the spectrum of the monoanion. The frequency of the $\nu_s(COO^-)$ mode is also shifted lower, and the combination $\nu$(OC−OH) + $\delta$(C−O−H) mode decreases significantly in intensity, revealing two medium intensity bands at 1278 and 1254 cm$^{-1}$ assigned to $\delta$(O═C−O$^-$) modes of the carboxylate group. At pH 7.8, a weak band at 1100 cm$^{-1}$ is observed that is assigned to the $\nu_s$(C−OH) mode of the hydroxyl group.

Upon complexation with uranyl, the vibrational spectrum of citrate changes significantly from that of the free ligand. At pH 4.1 where $[(UO_2)_2Cit_2]^{2-}$ predominates (Figure 5a), the presence of the $\nu_s$(C═O) band at 1730 cm$^{-1}$ confirms the presence of free, protonated carboxylic acid groups in the complex. The increase in frequency of this mode relative to that of the citrate monoanion at pH 4.0 may be due to disruption of intramolecular hydrogen bonding with concomitant strengthening of the C═O bond upon complex formation. The $\nu_{as}(COO^-)$ and $\nu_s(COO^-)$ modes appear at 1579 and 1382 cm$^{-1}$, respectively. Bands of medium intensity associated with $\delta$(O═C−O$^-$) vibrations appear at 1236 and 1207 cm$^{-1}$, and the hydroxyl $\nu_s$(C−OH) now appears as a sharp band at 1085 cm$^{-1}$. The $H_2O$ libration band absorbs strongly below 1000 cm$^{-1}$, making it difficult to obtain quality spectra in this region. However, a band due to $\nu_{as}(UO_2)$ is observed at 919 cm$^{-1}$.

At higher pH values, the $[(UO_2)_3Cit_3]^{3-}$ and $(UO_2)_3Cit_2$ complexes coexist, making the IR spectra in Figure 5b,c

**Table 1.** IR Peak Frequencies (in $cm^{-1}$) and Assignments for Aqueous Species

| pH, citrate species | | | | pH, uranyl/citrate species | | | |
|---|---|---|---|---|---|---|---|
| 2.1, $H_3Cit$ | 4.0, $H_2Cit^-$ | 5.5, $HCit^{2-}$ | 7.8, $Cit^{3-}$ | 4.0, $[(UO_2)_2Cit_2]^{2-}$ | 7.8, $[(UO_2)_3Cit_3]^{3-}$ | 7.6, $(UO_2)_3Cit_2$ | assignment[a] |
| 1724 | 1721 | 1725 | | 1730 | | | $\nu_s$(C═O) |
| | 1583 | 1568 | 1565 | 1579 | 1564 | 1566 | $\nu_{as}(COO^-)$ |
| | | | | 1411sh | | | |
| | | | | | | 1455sh | |
| | | 1440sh | 1438sh | | 1429sh | 1420sh | $\gamma(CH_2)$ |
| | 1397 | 1391 | 1389 | | 1393 | 1378 | $\nu_s(COO^-)$ |
| | | | | 1382 | 1374sh | | $\nu_s(COO^-)$ |
| | | | | | | 1296 | |
| 1223 | 1220 | | | | | | $\nu$(OC−OH) + $\delta$(C−O−H) |
| | | 1279 | 1278 | | | 1278 | $\delta$(O═C−$O^-$) |
| | | | | 1236 | 1242 | 1246 | $\delta$(O═C−$O^-$) |
| | | | 1254 | 1207 | 1211 | 1214 | $\delta$(O═C−$O^-$) |
| | | | 1100 | 1085 | 1103 | 1104 | $\nu$(C−OH) |
| | | | | | 1067 | | $\nu$(C−OH) |
| | | | | 919 | 891 | 888 | $\nu_{as}(UO_2)$ |

[a] $\nu$ = stretch; $\nu_s$ = symmetric stretch; $\nu_{as}$ = asymmetric stretch; $\delta$ = deformation; sh = shoulder.

somewhat more difficult to interpret. At pH 7.8 and a 1:1 uranyl/citrate ratio (Figure 5b), $[(UO_2)_3Cit_3]^{3-}$ predominates. On the basis of the relative areas of the 812 and 795 $cm^{-1}$ $\nu_s(UO_2)$ modes in the Raman spectrum at pH 7.8, the relative amount of $(UO_2)_3Cit_2$ is estimated to be ~25% of the sum of these two species. The $\nu_{as}(COO^-)$ mode at this pH appears at 1564 $cm^{-1}$, ~15 $cm^{-1}$ lower than its position for $[(UO_2)_2Cit_2]^{2-}$. The $\nu_s(COO^-)$ mode has split into a sharp peak at 1393 $cm^{-1}$ and a shoulder at ~1374 $cm^{-1}$, indicating the presence of two discrete $COO^-$ environments. Two modes due to $\delta$(O═C−$O^-$) appear at 1242 and 1211 $cm^{-1}$, only slightly shifted from their positions in the spectrum of $[(UO_2)_2Cit_2]^{2-}$. The hydroxyl $\nu_s$(C−OH) splits into two modes at 1103 and 1067 $cm^{-1}$, possibly indicating two OH conformations. The $\nu_{as}(UO_2)$ mode appears at 891 $cm^{-1}$. At pH 7.6 and a 3:2 uranyl/citrate ratio (Figure 5c), $(UO_2)_3Cit_2$ predominates, with the $[(UO_2)_3Cit_3]^{3-}$ complex contributing ~40% to the spectrum. In this spectrum, $\nu_s(COO^-)$ appears as one broad band with a maximum at 1378 $cm^{-1}$ with weak shoulders at ~1420 and 1455 $cm^{-1}$. The shoulder at ~1420 $cm^{-1}$ may be related to a $CH_2$ deformation mode, but the weaker shoulder at 1455 $cm^{-1}$ remains unassigned. The $\delta$(O═C−$O^-$) modes are essentially unchanged at 1246 and 1214 $cm^{-1}$, but weak modes now appear at 1296 and 1278 $cm^{-1}$. A single hydroxyl $\nu_s$(C−OH) mode appears at 1104 $cm^{-1}$, and the $\nu_{as}(UO_2)$ mode is observed at 888 $cm^{-1}$.

**ESI-MS.** The ability to generate gas-phase ions from solution species makes ESI-MS extremely valuable for the study of labile, solution-phase species important in environmental and biological processes. ESI-MS is increasingly used to examine both metal ion speciation in aqueous solution and metal−ligand stoichiometry and structure.[29−34] ESI-MS is used here to corroborate the number and stoichiometries of the $UO_2^{2+}$−citrate complexes in solution and to confirm results from Raman spectroscopy. Mass spectra acquired for the $UO_2^{2+}$−citrate system as a function of pH and uranyl/citrate ratio are shown in Figure 7a−e.

Figure 7a shows the positive ion spectrum of a solution 0.5 mM each in uranyl and citrate at $^s_w$pH 4.0 (20% (v/v) acetonitrile/$H_2O$). At this pH and uranyl/citrate ratio, $[(UO_2)_2Cit_2]^{2-}$ predominates in solution. The $UO_2^{2+}$ groups in the complex each carry a +2 charge, while the citrate ligands carry a −3 charge when fully deprotonated. Therefore, the dimer can be −1, −2, or neutral depending on the protonation state of the two free carboxyl groups. In positive ion mode, singly charged $Na^+$ and $NH_4^+$ adducts of $H_2[(UO_2)_2Cit_2]$ appear at *m*/*z* 956.2, 961.3, 1024.4, and 1046.2 (Figure 7a, Table 2), indicating that in the gas phase the dimer COOH groups are fully protonated. Since gas-phase protonation state is a function of gas-phase proton affinity and not necessarily related to the strength of an acid relative to $H_2O$ in aqueous solution,[35] the protonation state of the complex in solution at pH 4.0 cannot be directly inferred from this result. When the counterion in solution is $Cl^-$ instead of $NO_3^-$ (Figure 7b), the intense peak at *m*/*z* 1024.4 corresponding to $[H_2(UO_2)_2Cit_2 + H_2O + Na + HNO_3]^+$ is replaced by an intense peak at *m*/*z* 997.4 due to the corresponding HCl adduct $[H_2(UO_2)_2Cit_2 + H_2O + Na + HCl]^+$, while the weak signal at 1046.2 from the $[H(UO_2)_2Cit_2 + H_2O + 2Na + HNO_3]^+$ species disappears. A signal at *m*/*z* 1002.3 is observed consistently in all spectra at $^s_w$pH 4 with both $NO_3^-$ and $Cl^-$ as counterions. It appears irreproducibly in spectra at $^s_w$pH ~ 7.5. Although tentative at this point, this species is assigned to $[H_2(UO_2)_2Cit_2 + 2H_2O + 2Na]^+$ in which one uranium atom in the complex is reduced from the +6 to the +5 oxidation state. The reduction of complexed metal ions by redox processes

(29) Ross, A. R. S.; Ikonomou, M. G.; Thompson, J. A. J.; Orians, K. J. *Anal. Chem.* **1998**, *70*, 2225−2235.
(30) Moulin, C.; Charron, N.; Plancque, G.; Virelizier, H. *Appl. Spectrosc.* **2000**, *54*, 843−848.
(31) Spasojevic, I.; Boukhalfa, H.; Stephens, R. D.; Crumbliss, A. L. *Inorg. Chem.* **2001**, *40*, 49−58.
(32) Gianelli, L.; Amendola, V.; Fabbrizzi, L.; Pallavicini, P.; Mellerio, G. G. *Rapid Commun. Mass Spectrom.* **2001**, *15*, 2347−2353.
(33) Mineo, P.; Vitalini, D.; Mendola, D. L.; Rizzarelli, E.; Scamporrino, E.; Vecchio, G. *Rapid Commun. Mass Spectrom.* **2002**, *16*, 722−729.
(34) Neubert, H.; Hider, R. C.; Cowan, D. A. *Rapid Commun. Mass Spectrom.* **2002**, *16*, 1556−1561.
(35) Cech, N. B.; Enke, C. G. *Mass Spectrom. Rev.* **2001**, *20*, 362−387.

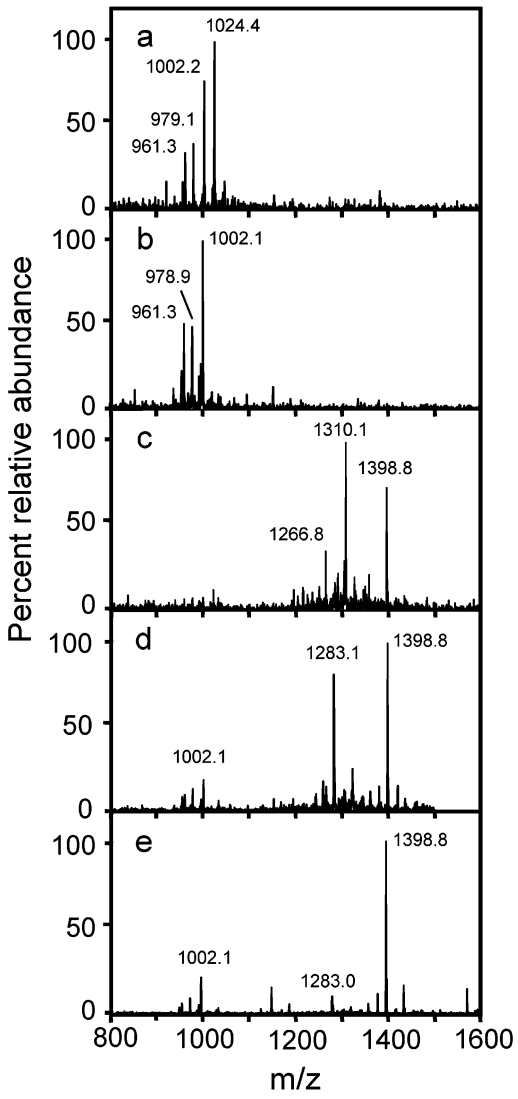


**Figure 7.** Positive ion mass spectra of the $UO_2^{2+}$/citrate system: (a) 1:1 uranyl/citrate in 20% acetonitrile/$H_2O$ at ${}^{s}_{w}$pH 4.0, $NO_3^-$, (b) 1:1 uranyl/citrate in 20% acetonitrile/$H_2O$ at ${}^{s}_{w}$pH 4.0, $Cl^-$, (c) 3:2 uranyl/citrate in 20% acetonitrile/$H_2O$ at ${}^{s}_{w}$pH 7.6, $NO_3^-$, (d) 3:2 uranyl/citrate in 20% acetonitrile/$H_2O$ at ${}^{s}_{w}$pH 7.6, $Cl^-$, (e) 1:1 uranyl/citrate in 20% acetonitrile/$H_2O$ at ${}^{s}_{w}$pH 7.8, $Cl^-$.

occurring during the electrospray process or by reactions occurring in the gas phase is commonly seen in ESI-MS, but is not completely understood.[32,36−39] A more detailed discussion of the gas-phase behavior of the $UO_2^{2+}$−citrate complexes will be provided in a forthcoming publication.[40]

The Raman spectral data show that, at pH values $>\sim$5, both $[(UO_2)_3Cit_3]^{3-}$ and $(UO_2)_3Cit_2$ coexist, and that their respective abundances in solution can be controlled through manipulation of the uranyl/citrate ratio. Predictably, this same behavior is observed in the results from ESI-MS. Figure 7c−e shows the effect of changing the uranyl/citrate ratio on the ESI mass spectrum at ${}^{s}_{w}$pH 7.6. At a 3:2 uranyl/citrate ratio (0.6 mM in uranyl and 0.4 mM in citrate, 20% (v/v) acetonitrile/$H_2O$), three peaks at *m*/*z* 1266.8, 1310.1, and 1398.8 corresponding to singly charged ions appear (Figure 7c). The ion at *m*/*z* 1310.1 is assigned to $[(UO_2)_3Cit_2 + HNO_3 + 2H_2O + Na]^+$. When $Cl^-$ is used as a counterion in place of $NO_3^-$, the corresponding HCl adduct, $[(UO_2)_3Cit_2 + HCl + 2H_2O + Na]^+$, appears at *m*/*z* 1283.1 (Figure 7d). The ion at *m*/*z* 1266.8 remains unassigned and may be produced in a manner similar to the *m*/*z* 1002.2 ion already discussed. The signal at *m*/*z* 1398.8 seen in Figure 7c,d corresponds to the singly charged $[H_3(UO_2)_3Cit_3 + H_2O + H]^+$ ion. At a 1:1 uranyl/citrate ratio (0.5 mM in uranyl and 0.5 mM in citrate, 20% (v/v) acetonitrile/$H_2O$), the relative abundance of this ion increases dramatically, with a concomitant decrease in the abundance of the $[(UO_2)_3Cit_2 + HCl + 2H_2O + Na]^+$ species (Figure 7e). Small peaks at *m*/*z* 1380.8 and 1436.6 correspond to $[H_3(UO_2)_3Cit_3 + H]^+$ and $[H_3(UO_2)_3Cit_3 + H_2O + K]^+$ ions, respectively. The $H_3(UO_2)_3Cit_3$ species is extremely stable in the gas phase.

The ESI mass spectra in Figure 8a−e show the effect of very small changes in the uranyl/citrate ratio on the relative abundances of the $(UO_2)_3Cit_2$ and $[(UO_2)_3Cit_3]^{3-}$ species. The relative abundance of the $(UO_2)_3Cit_2$ adduct at *m*/*z* 1283.1 increases systematically with an increase in the uranyl/citrate ratio. In addition, new species, most likely also adducts of $(UO_2)_3Cit_2$, appear at *m*/*z* 1242.7, 1260.0, 1320.5, and 1360.9, respectively. The trend of increasing $(UO_2)_3Cit_2$ in the gas phase corresponds to a similar increase occurring in solution, as can be seen by comparison of the ESI mass spectra in Figure 8a−e with the corresponding Raman spectra in Figure 8f−j. In the Raman spectra, the intensity of $\nu_s(UO_2)$ at 812 $cm^{-1}$ increases with this ratio, indicating an increase in the concentration of $(UO_2)_3Cit_2$, with a concomitant decrease in intensity of the $\nu_s(UO_2)$ at 795 $cm^{-1}$ from $[(UO_2)_3Cit_3]^{3-}$. These data clearly indicate that the formation of $(UO_2)_3Cit_2$ is favored when citrate is limiting. The existence of this species in solution has important ramifications, since its formation precludes the hydrolysis and subsequent sequestering of uranyl in the form of surface-associated $UO_2$ mineral phases, thereby enhancing the solubility of uranyl even at low citrate concentrations.

The 20% (v/v) acetonitrile/$H_2O$ mixture was used in the described ESI-MS experiments because the presence of acetonitrile in solution increases the electrospray ionization efficiency. However, the addition of acetonitrile decreases the value of the dielectric constant from 78.5 in $H_2O$ at 25 °C[41] to 70.1 in a 20% (v/v) acetonitrile/$H_2O$ mixture at 25 °C.[25] This may have the effect of increasing long-range electrostatic interactions in solution, thereby slightly increasing the stability constants of the uranyl/citrate complexes. In addition, specific interactions between acetonitrile and solute molecules may induce a change in the $\Delta G$ of complex formation. The overall effect of a decrease in dielectric

(36) Gatlin, C. L.; Turecek, F.; Vaisar, T. *Anal. Chem.* **1994**, *66*, 3950−3958.
(37) Colton, R.; D'Agostino, A.; Traeger, J. C. *Mass. Spectrom. Rev.* **1995**, *14*, 79−106.
(38) Vaisar, T.; Gatlin, C. L.; Turecek, F. *Int. J. Mass. Spectrom. Ion. Processes* **1997**, *162*, 77−87.
(39) Lavanant, H.; Virelizier, H.; Hoppilliard, Y. *J. Am. Soc. Mass. Spectrom.* **1998**, *9*, 1217−1221.
(40) Pasilis, S. P.; Somogyi, A.; Pemberton, J. E. To be submitted.
(41) Fernandez, D. P.; Mulev, Y.; Goodwin, A. R. H.; Sengers, J. M. H. L. *J. Phys. Chem. Ref. Data* **1995**, *24*, 33−69.

**Table 2.** ESI-MS Peak Assignments for $UO_2^{2+}$−Citrate Complexes

| | | $UO_2^{2+}$−citrate complex stoichiometry (pH) | | | | | |
|---|---|---|---|---|---|---|---|
| | | $[(UO_2)_2Cit_2]^{3-}$ ($^{s}_{w}$pH 4.0) | | $[(UO_2)_3Cit_3]^{3-}$ ($^{s}_{w}$pH 7.6) | | $(UO_2)_3Cit_2$ ($^{s}_{w}$pH 7.6) | |
| species | calcd *m*/*z* | obsd *m*/*z*[a] | % rel abund | obsd *m*/*z* | % rel abund | obsd *m*/*z* | % rel abund |
| $[H_2(UO_2)_2Cit_2 + NH_4]^+$ | 938.1 | 938.5 | 17 | | | | |
| $[H_2(UO_2)_2Cit_2 + H_2O + NH_4]^+$ | 956.1 | 956.2 | 16 | | | | |
| $[H_2(UO_2)_2Cit_2 + H_2O + Na]^+$ | 961.1 | 961.3 | 34 | | | | |
| $[H_2(UO_2)_2Cit_2 + 2H_2O + Na]^+$ | 979.1 | 979.1 | 39 | | | | |
| | 1002.1 | 1002.3 | 77 | | | | |
| $[H_2(UO_2)_2Cit_2 + HNO_3 + H_2O + Na]^+$ | 1024.2 | 1024.4 | 100 | | | | |
| $[H(UO_2)_2Cit_2 + HNO_3 + H_2O + 2Na]^+$ | 1046.1 | 1046.2 | 16 | | | | |
| | | | | | | 1266.8 | 35 |
| $[(UO_2)_3Cit_2 + HCl + 2H_2O + Na]^+$ | 1283.1 | | | | | 1283.1 | 82 |
| $[(UO_2)_3Cit_2 + HNO_3 + 2H_2O + Na]^+$ | 1310.2 | | | | | 1310.1 | 100 |
| $[H_3(UO_2)_3Cit_3 + H]^+$ | 1381.2 | | | 1380.8 | 6.3 | | |
| $[H_3(UO_2)_3Cit_3 + H_2O + H]^+$ | 1399.2 | | | 1398.8 | 100 | 1398.8 | 74 |
| $[H_3(UO_2)_3Cit_3 + H_2O + K]^+$ | 1437.1 | | | 1436.6 | 7.4 | | |

[a] Peaks over 15% relative abundance.

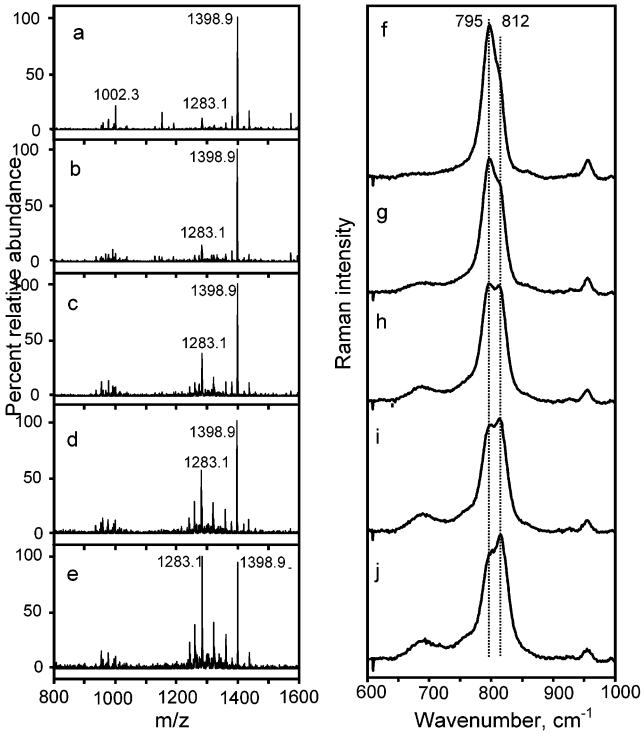


**Figure 8.** (a−e) Positive ion mass spectra of the $UO_2^{2+}$−citrate system showing effect of variation in uranyl/citrate ratio. All samples in 20% acetonitrile/$H_2O$ at $^{s}_{w}$pH 7.8: (a) 1:1 (0.5 mM uranyl, 0.5 mM citrate), (b) 1.2:1 (0.54 mM uranyl, 0.45 mM citrate), (c) 1.4:1 (0.58 mM uranyl, 0.42 mM citrate), (d) 1.5:1 (0.60 mM uranyl, 0.40 mM citrate), (e) 1.7:1 (0.63 mM uranyl, 0.37 mM citrate). (f−j) Raman spectra of the $UO_2^{2+}$−citrate system showing effect of variation in uranyl/citrate ratio. All samples in $H_2O$ at pH 7.7: (f) 1:1 (50 mM uranyl, 50 mM citrate), (g) 1.2:1 (54 mM uranyl, 45 mM citrate), (h) 1.4:1 (58 mM uranyl, 42 mM citrate), (i) 1.5:1 (60 mM uranyl, 40 mM citrate), (j) 1.7:1 (63 mM uranyl, 37 mM citrate).

constant and a change in $\Delta G$ cannot be known without further investigation.

The ESI-MS data corroborate earlier conclusions about the existence of the $[(UO_2)_2Cit_2]^{2-}$ species[12,13,15] and provide definitive evidence for the existence of two high-pH species, $(UO_2)_3Cit_2$ and $[(UO_2)_3Cit_3]^{3-}$, proposed from titrimetric and spectrophotometric studies,[8] and from Raman spectroscopy (this work). Unfortunately, definitive structures cannot be proposed for these species from spectral data alone.

## Conclusions

A detailed spectroscopic examination of the pH-dependent behavior of the $UO_2^{2+}$−citrate system in aqueous solution is presented. Raman and ATR-FTIR spectroscopies and ESI-MS have proven to be powerful tools in combination for elucidation of the equilibrium distribution of $UO_2^{2+}$−ligand complexes. The results presented here show definitive evidence for three structurally distinct $UO_2^{2+}$−citrate complexes that exist in dynamic equilibrium over an environmentally relevant pH range. Citrate is a common constituent of soils and is clearly important to the equilibrium distribution of uranium in aqueous solution at environmentally relevant pH values. The pH-induced structural changes of the uranyl−citrate species described here allow a better understanding of previously observed phenomena such as the pH dependence of $UO_2^{2+}$−citrate complex biodegradation [3,42] and photodegradation, [43,44] both of which are processes under investigation for the remediation of uranium in soils.[3,42,44,45] Furthermore, the strength of the $UO_2^{2+}$−citrate interaction is such that the formation of insoluble uranium(VI) oxides is precluded if the concentration of citrate is approximately equal to that of uranyl.

**Acknowledgment.** We gratefully acknowledge the Idaho National Engineering and Environmental Laboratory for financial support of this research. We also thank Dr. Arpad Somogyi of the University of Arizona Mass Spectrometry Facility for assistance with the ESI-MS experiments and data interpretation.

IC0341800

(42) Francis, A. J.; Dodge, C. J.; Gillow, J. B. *Nature* **1992**, *356*, 140−142.
(43) Ohyosi, A.; Ueno, K. *J. Inorg. Nucl. Chem.* **1974**, *36*, 379−384.
(44) Dodge, C. J.; Francis, A. J. *Environ. Sci. Technol.* **1994**, *28*, 1300−1306.
(45) Dodge, C. J.; Francis, A. J. *Environ. Sci. Technol.* **2002**, *36*, 2094−2100.